

# Maximal energy that can be converted by a dielectric elastomer generator

Soo Jin Adrian Koh,<sup>1,2</sup> Xuanhe Zhao,<sup>2</sup> and Zhigang Suo<sup>2,a)</sup>

<sup>1</sup>Institute of High Performance Computing Fusionopolis Way, 16-16 Connexis, Singapore 138632, Singapore

<sup>2</sup>School of Engineering and Applied Sciences, Harvard University, Cambridge, Massachusetts 02138, USA

(Received 27 May 2009; accepted 10 June 2009; published online 30 June 2009)

Mechanical energy can be converted to electrical energy by using a dielectric elastomer generator. The elastomer is susceptible to various modes of failure, including electrical breakdown, electromechanical instability, loss of tension, and rupture by stretch. The modes of failure define a cycle of maximal energy that can be converted. This cycle is represented on planes of work-conjugate coordinates and may be used to guide the design of practical cycles. © 2009 American Institute of Physics. [DOI: 10.1063/1.3167773]

Diverse technologies are being developed to harvest energy from renewable sources.<sup>1-3</sup> This letter focuses on one particular technology: dielectric elastomer (DE) generators.<sup>4-8</sup> When a membrane of a DE is prestretched and precharged, a reduction in the tensile force under the open-circuit condition increases the voltage (Fig. 1). Thus, a cycle can be designed to convert mechanical energy into electrical energy. Experiments have shown that DEs can convert energy up to 0.4 J/g, which is at least an order of magnitude higher than the specific energies of piezoelectric ceramics and electromagnetic generators.<sup>5</sup> DE generators have been designed to harvest energy from walking,<sup>5,6</sup> ocean waves,<sup>7</sup> wind, and combustion.<sup>8</sup> These generators are lightweight, compliant, and rust-free, allowing them to be deployed widely.

This letter describes a method to calculate the maximal energy that can be converted by a DE generator. The elastomer is susceptible to various modes of failure.<sup>9,10</sup> We use these modes of failure to define a cycle on the force-displacement plane and the voltage-charge plane. The area enclosed by the cycle gives the maximal energy of conversion. Such a diagram may be used to guide the design of practical cycles.

Our method is based on a nonlinear theory of elastic dielectrics.<sup>11-18</sup> With reference to Fig. 1, consider a membrane of a DE, of sides  $L_1$ ,  $L_2$ , and  $L_3$  in its undeformed state. The two faces of the membrane are coated with compliant electrodes. When the electrodes are subject to a voltage  $\Phi$  and the membrane is subject to forces  $P_1$  and  $P_2$ , the electrodes gain charges  $+Q$  and  $-Q$ , and the membrane deforms to a state of sides  $\lambda_1 L_1$ ,  $\lambda_2 L_2$ , and  $\lambda_3 L_3$ , where  $\lambda_1$ ,  $\lambda_2$ , and  $\lambda_3$  are the stretches of the membrane in the three directions. The membrane is taken to be incompressible, so that  $\lambda_1 \lambda_2 \lambda_3 = 1$ . Define the nominal stresses by  $s_1 = P_1 / L_2 L_3$  and  $s_2 = P_2 / L_1 L_3$ , the nominal electric field by  $\tilde{E} = \Phi / L_3$ , and the nominal electric displacement by  $\tilde{D} = Q / L_1 L_2$ . By contrast, the true stresses  $\sigma_1$  and  $\sigma_2$ , the true electric field  $E$ , and the true electric displacement  $D$  are the same quantities divided by the dimensions of the membrane in the deformed state. The true quantities relate to the nominal ones as  $\sigma_1 = s_1 \lambda_1$ ,  $\sigma_2 = s_2 \lambda_2$ ,  $E = \tilde{E} \lambda_1 \lambda_2$ , and  $D = \tilde{D} \lambda_1^{-1} \lambda_2^{-1}$ .

To illustrate essential ideas, consider the case where the membrane is subject to equal biaxial forces, so that  $s_1 = s_2 = s$  and  $\lambda_1 = \lambda_2 = \lambda$ . The membrane is taken to deform under an isothermal condition, and the temperature will not be considered explicitly. Consequently, the membrane is a thermodynamic system of two independent variations. The variations can be described by two independent variables of many choices. Once chosen, the two independent variables can be used as the coordinates of a plane, with each point in the plane representing a state of the system. To calculate the energy of conversion, we choose planes of work-conjugate coordinates: either the force-displacement plane or the voltage-charge plane (Fig. 2). A design of a generator may be represented by a cycle on either plane. The amount of mechanical energy converted to electrical energy is the area enclosed by the cycle on the voltage-charge plane. The same energy is twice the area enclosed by the cycle on the force-displacement plane, because equal biaxial forces have been assumed.

We prescribe the equations of state by using the model of ideal DE.<sup>19</sup> The elastomer is a network of polymers with a low density of crosslinks, so that deformation affects polarization negligibly. This model has been used almost exclusively in the literature on DEs; see Ref. 20 for a review. For an ideal DE subject to a biaxial stress  $s$  and electric field  $\tilde{E}$ , the equations of state are<sup>21</sup>

$$s/\mu = \lambda - \lambda^{-5} - (\tilde{D}^2/\varepsilon\mu)\lambda^{-5}, \tag{1}$$

$$\tilde{E}/\sqrt{\mu/\varepsilon} = (\tilde{D}/\sqrt{\varepsilon\mu})\lambda^{-4}, \tag{2}$$

where  $\mu$  is the modulus and  $\varepsilon$  is the permittivity. In numerical calculations, we assume that  $\mu = 10^6$  N/m<sup>2</sup> and  $\varepsilon = 3.54 \times 10^{-11}$  F/m.

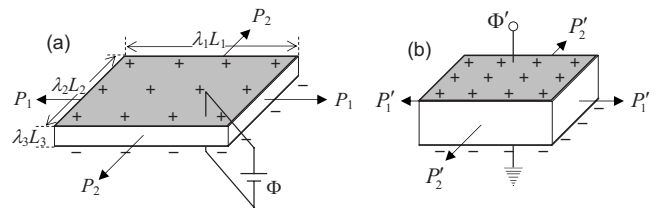


FIG. 1. (a) A membrane of a DE is prestretched and precharged. (b) After the elastomer is switched to an open circuit, as the tensile force reduces, the elastomer increases thickness and decreases the capacitance, so that the voltage increases.

<sup>a)</sup>Electronic mail: suo@seas.harvard.edu.

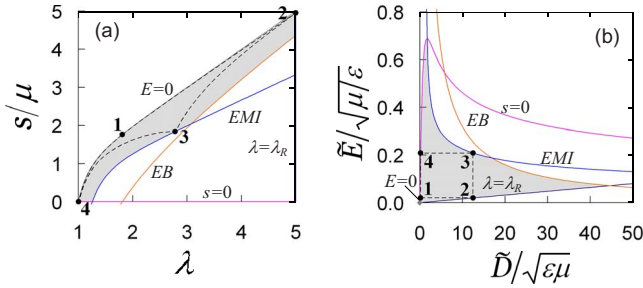


FIG. 2. (Color online) A thermodynamic state of the membrane is represented by (a) a point in the force-displacement plane or (b) a point in the voltage-charge plane. The stress-stretch curve for an uncharged membrane is marked by  $E=0$ . Also plotted are various modes of failure: EB, EMI, loss of tension ( $s=0$ ), and rupture by stretch ( $\lambda=\lambda_R$ ).

When the membrane is uncharged,  $\tilde{D}=0$  and  $\tilde{E}=0$ , Eq. (1) becomes that

$$s/\mu = \lambda - \lambda^{-5}. \quad (3)$$

On the force-displacement plane in Fig. 2, this curve sets the upper bound: any charge on the electrodes would reduce the tensile stress at a fixed stretch. On the voltage-charge plane, the condition  $\tilde{D}=0$  and  $\tilde{E}=0$  corresponds to the origin.

Subject to an electric field, the elastomer may fail by electrical breakdown (EB). The microscopic process of EB can be complex, and will not be studied in this paper. Here we assume that EB occurs when the true electric field  $E$  reaches a critical value  $E_{EB}$ . Thus, breakdown occurs at the nominal electric field  $\tilde{E}=E_{EB}\lambda^{-2}$ , so that Eqs. (1) and (2) become

$$s/\mu = \lambda - \lambda^{-5} - [E_{EB}^2/(\mu/\varepsilon)]\lambda^{-1}, \quad (4)$$

$$\tilde{E}/\sqrt{\mu/\varepsilon} = [E_{EB}^2/(\mu/\varepsilon)][\tilde{D}/\sqrt{\varepsilon\mu}]^{-1}. \quad (5)$$

Figure 2 plots in the two planes these conditions for EB, assuming a value reported in Ref. 22,  $E_{EB}=3 \times 10^8$  V/m.

Prior to EB, as the voltage is increased, the elastomer reduces thickness, so that the positive feedback between a thinner elastomer and a higher true electric field may result in electromechanical instability (EMI).<sup>21-26</sup> The critical condition for the instability can be obtained as follows. Eliminate  $\tilde{D}$  from Eqs. (1) and (2) and express  $\tilde{E}$  as a function of  $\lambda$  and  $s$ . At a constant  $s$  the function  $\tilde{E}(\lambda, s)$  reaches a maximum when

$$s/\mu = (2/3)(\lambda - 4\lambda^{-5}). \quad (6)$$

This maximum nominal electric field corresponds to the critical voltage for the onset of the EMI. A combination of Eqs. (1), (2), and (6) gives that

$$\tilde{E}/\sqrt{\mu/\varepsilon} = (\tilde{D}/\sqrt{\varepsilon\mu})[3(\tilde{D}^2/\varepsilon\mu) - 5]^{-2/3}. \quad (7)$$

Figure 2 plots in the two planes the critical conditions (6) and (7).

To avoid excessively high voltage in use, the membrane must be thin. The thin membrane, however, buckles under slight compressive stresses in its plane. Even for a pre-tensioned membrane, the voltage induces deformation, which may remove the tensile prestress, a condition known as *loss of tension*. This condition  $s=0$  together with Eqs. (1) and (2), gives that

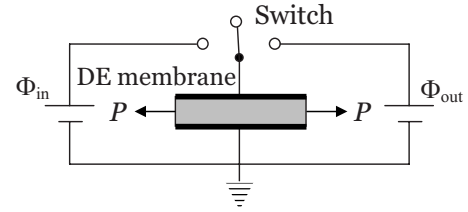


FIG. 3. A circuit that enables a mechanical force to pump electric charge from a low-voltage battery to a high-voltage battery.

$$\tilde{E}/\sqrt{\mu/\varepsilon} = (\tilde{D}/\sqrt{\varepsilon\mu})[1 + (\tilde{D}^2/\varepsilon\mu)]^{-2/3}. \quad (8)$$

Figure 2 plots in the two planes the conditions for loss of tension.

When deformed severely, the membrane may *rupture by stretch*. The microscopic process of rupture can be complex. Here we assume that the membrane ruptures when the stretch reaches a critical value  $\lambda_R$ . Inserting this condition to Eq. (2), we obtain that

$$\tilde{E}/\sqrt{\mu/\varepsilon} = (\tilde{D}/\sqrt{\varepsilon\mu})\lambda_R^{-4}. \quad (9)$$

Experiments have suggested  $\lambda_R \leq 6$  for equal biaxial stretch.<sup>9</sup> We use a value of  $\lambda_R=5$  in our calculations. Figure 2 plots in the two planes the conditions for rupture by stretch.

On either plane in Fig. 2, various modes of failure enclose a shaded area of allowable states: a state inside the area will not fail by any modes, but a state outside the area will fail by one or more of the modes. One may refine the critical condition for each mode of failure, or add other modes. For example, EB is a complex phenomenon and using a fixed value for the breakdown field is an oversimplification. Breakdown fields may vary with the thickness and pre-stretch. These refinements will alter the shaded areas in Fig. 2, but will not change the qualitative considerations.

The shaded area enclosed by various modes of failure defines the maximal energy of conversion. Using the representative material parameters indicated above, and the mass density of  $\rho=1000$  kg/m<sup>3</sup>, we find that the maximal specific energy is 6.3 J/g. This maximal-energy cycle, however, may be difficult to realize in practice. For example, when the state of the generator travels along the lines of EB and EMI, the voltage must be precisely tuned. Nonetheless, the maximal-energy cycle sets an upper bound of the energy that can be converted by DE generators.

To illustrate a procedure to design practical cycles, consider a cycle that requires two batteries: one supplies charge at a low voltage  $\Phi_{in}$ , and the other stores charge at a high voltage  $\Phi_{out}$  (Fig. 3). A switch can connect the elastomer to the input battery, or connect the elastomer to the output battery, or keep the elastomer in an open circuit. After each cycle, the mechanical force pumps certain amount of electric charge from the low-voltage battery to the high-voltage battery. This cycle is represented by a rectangle on the voltage-charge plane in Fig. 2, with top and bottom sides set by  $\Phi_{out}$  and  $\Phi_{in}$ , and the left and right sides set by  $Q_{low}$  and  $Q_{high}$ . The same cycle of operation is also represented by the dashed curves on the force-displacement plane.

From state 1 to state 2, the elastomer is switched to the input battery, and is pulled from a small stretch up to the stretch of rupture. During this process, the elastomer reduces

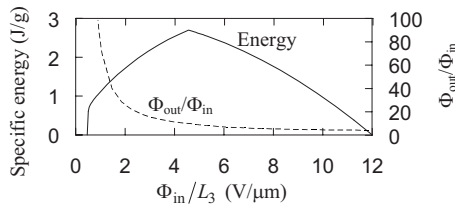


FIG. 4. Specific energy and amplification of voltage ( $\Phi_{\text{out}}/\Phi_{\text{in}}$ ) for cycles represented by various rectangles in Fig. 2.

the thickness and increases the capacitance, drawing charge from the input battery, such that the charge on the electrodes increases from  $Q_{\text{low}}$  to  $Q_{\text{high}}$ .

From state 2 to state 3, the elastomer is switched to an open circuit, and the tensile force is reduced, allowing the elastomer to thicken until it is close to EMI. During this process, the charge on the electrodes is kept at  $Q_{\text{high}}$  and the voltage between the electrodes increases from  $\Phi_{\text{in}}$  to  $\Phi_{\text{out}}$ .

From state 3 to state 4, the elastomer is switched to the output battery, and the tensile force is further reduced until the condition of loss of tension. During the process, the elastomer increases the thickness and reduces the capacitance, transferring charge to the output battery, such that the charge on the electrodes decreases from  $Q_{\text{high}}$  to  $Q_{\text{low}}$ .

From state 4 back to state 1, the elastomer is once again switched to an open circuit, and the tensile force is increased, allowing the elastomer to reduce the thickness. During this process, the charge on the electrodes is kept at  $Q_{\text{low}}$ , and the voltage between the electrodes reduces from  $\Phi_{\text{out}}$  to  $\Phi_{\text{in}}$ . The cycle then repeats itself.

On the voltage-charge plane in Fig. 2, rectangles of different aspect ratios can be selected by varying state 2 along the line  $\lambda = \lambda_R$ . Once state 2 is selected, we fit the largest rectangle within the shaded area. Figure 4 plots the specific energy generated per cycle of operation, and amplification of voltage for various rectangles. The specific energy is a maximum when state 3 falls on the intersection of the lines of EB and EMI. Figure 4 also shows the tradeoff between the specific energy and the amplification of voltage.

In summary, we have described a method to analyze electromechanical cycles for energy harvesting. We represent the states of a DE by points in planes of work-conjugating coordinates. Various modes of failure define a cycle of maximal energy of conversion. Diagrams of this kind can also be used to guide the design of practical cycles.

This work is funded by the Agency for Science, Technology and Research A\*STAR, Singapore, through the sponsoring of a two-year postdoctoral visit of S.J.A.K. to Harvard University and by the National Science Foundation through a grant on Soft Active Materials (Contract No. CMMI-0800161).

- <sup>1</sup>P. D. Mitcheson, E. M. Yeatman, G. K. Rao, A. S. Holmes, and T. C. Green, *Proc. IEEE* **96**, 1457 (2008).
- <sup>2</sup>T. Starner and J. A. Paradiso, *Low Power Electronics Design* (CRC, Boca Raton, 2004), Chap. 7, p. 45-1; <http://www.media.mit.edu/resenv/pubs/books/Starner-Paradiso-CRC.1.452.pdf>.
- <sup>3</sup>J. A. Paradiso and T. Starner, *IEEE Pervasive Comput.* **4**, 18 (2005); <http://www.compute.org/pervasive>.
- <sup>4</sup>F. Carpi, D. De Rossi, R. Kornbluh, R. Pelrine, and P. Sommer-Larsen, *Dielectric Elastomers as Electromechanical Transducers* (Elsevier, New York, 2008).
- <sup>5</sup>R. Pelrine, R. Kornbluh, J. Eckerle, P. Jeuck, S. Oh, Q. Pei, and S. Stanford, Proceedings of the SPIE Electroactive Polymer Actuators and Devices, Newport Beach, CA, March 2001 (unpublished), Vol. 4329, p. 148.
- <sup>6</sup>W. H. McKnight and W. C. McGinnis, U.S. Patent No. 6,433,465 (13 August 2002).
- <sup>7</sup>R. D. Kornbluh, R. E. Pelrine, H. Prahlaad, S. Chiba, J. S. Eckerle, B. Chavez, S. E. Stanford, and T. Low, U.S. Patent 2007/0257490 (8 November 2007).
- <sup>8</sup>H. Prahlaad, R. Kornbluh, R. Pelrine, S. Stanford, J. Eckerle, and S. Oh, Proceedings of the ISSS, Bangalore, India, 28–30 July 2005 (unpublished), Vol. SA-13, p. SA-100.
- <sup>9</sup>J. S. Plante and S. Dubowsky, *Int. J. Solids Struct.* **43**, 7727 (2006).
- <sup>10</sup>M. Moscardo, X. Zhao, Z. Suo, and Y. Lapusta, *J. Appl. Phys.* **104**, 093503 (2008).
- <sup>11</sup>A. Dorfmann and R. W. Ogden, *Acta Mech.* **174**, 167 (2005).
- <sup>12</sup>R. M. McMeeking and C. M. Landis, *J. Appl. Mech.* **72**, 581 (2005).
- <sup>13</sup>G. Kofod, W. Wirges, M. Paajanen, and S. Bauer, *Appl. Phys. Lett.* **90**, 081916 (2007).
- <sup>14</sup>Z. Suo, X. Zhao, and W. H. Greene, *J. Mech. Phys. Solids* **56**, 467 (2008).
- <sup>15</sup>R. Diaz-Calleja, M. J. Sanchis, and E. Riande, *J. Electrostat.* **67**, 158 (2009).
- <sup>16</sup>C. Trimarco, *Acta Mech.* **204**, 193 (2009).
- <sup>17</sup>D. K. Vu, P. Steinmann, and G. Possart, *Int. J. Numer. Methods Eng.* **70**, 685 (2007).
- <sup>18</sup>B. O'Brien, T. McKay, E. Calius, S. Xie, and I. Anderson, *Appl. Phys. A: Mater. Sci. Process.* **94**, 507 (2009).
- <sup>19</sup>X. Zhao, W. Hong, and Z. Suo, *Phys. Rev. B* **76**, 134113 (2007).
- <sup>20</sup>X. Zhao and Z. Suo, *J. Appl. Phys.* **104**, 123530 (2008).
- <sup>21</sup>X. Zhao and Z. Suo, *Appl. Phys. Lett.* **91**, 061921 (2007).
- <sup>22</sup>R. Pelrine, R. Kornbluh, Q. Pei, and J. Joseph, *Science* **287**, 836 (2000).
- <sup>23</sup>K. H. Stark and C. G. Garton, *Nature (London)* **176**, 1225 (1955).
- <sup>24</sup>A. N. Norris, *Appl. Phys. Lett.* **92**, 026101 (2008).
- <sup>25</sup>Y. J. Liu, L. W. Liu, Z. Zhang, L. Shi, and J. S. Leng, *Appl. Phys. Lett.* **93**, 106101 (2008).
- <sup>26</sup>M. Wissler and E. Mazza, *Sens. Actuators, A* **138**, 384 (2007).